Beyond spike-timing-dependent plasticity: a computational study of plasticity gradients across basal dendrites.

Jacopo Bono[1] , Claudia Clopath[1]

Abstract

Synaptic plasticity is thought to be the principal mechanism underlying learning in the brain. The majority of plastic networks in computational neuroscience combine point neurons with spike-timing-dependent plasticity (STDP) as the learning rule. However, a point neuron does not capture the complexity of dendrites. These long branches emanating from the soma allow non-linear local processing of the synaptic inputs. Furthermore, experimental evidence suggests that STDP is not the only learning rule available to neurons. Implementing a biophysically realistic neuron model, we wondered how dendrites allow for multiple synaptic plasticity mechanisms to coexist in a single cell. We show how a local, cooperative form of synaptic strengthening becomes increasingly powerful at larger distances from the soma, typically depending on dendritic spikes, explaining recent experimental results. The cooperative mechanism compensates the ineffectiveness of STDP on weak inputs and in distal parts of the dendrites, enhances the flexibility of a neuron by gating STDP, and allows for novel and robust associative learning schemes. Our work predicts that many plasticity rules increase the computational power of a neuron, and their implementation in future network models could be crucial to gain a deeper understanding of learning in the brain.

INTRODUCTION

Our brain continuously processes and stores novel information, providing us with a remarkable flexibility to adapt and learn in a continuously changing environment. Understanding which mechanisms underlie this plasticity is an important step towards understanding how sensory experience is processed in cortical areas. A seminal idea, now widely known as Hebb's postulate, suggested that synapses are the neurological substrates for learning [Hebb, 1949, Berlucchi and Buchtel, 2009]. In short, Hebb proposed that a neuron A persistently taking part in firing a neuron B, leads to increased synaptic efficacy from neuron A to B. Experiments later showed that high-frequency stimulation indeed evoked long-lasting increased efficacy, termed long-term potentiation (LTP), at hippocampal synapses [Bliss and Lømo, 1973]. Long-term depression (LTD), predicted as a mechanism to balance LTP [Stent, 1973, Bienenstock et al., 1982], was later shown to be evoked by low-frequency stimulation [Dudek and Bear, 1992].

A more complex picture of synaptic plasticity emerged, uncovering how the precise timing between the presynaptic and postsynaptic activity influences plasticity. When the presynaptic neuron fires just before the postsynaptic neuron, the synapse is potentiated. Instead, reversing the

[1]Department of Bioengineering, Imperial College London, South Kensington Campus, London SW7 2AZ, UK. Correspondence and requests for materials should be addressed to C.C. (email: c.clopath@imperial.ac.uk).

firing order leads to synaptic depression [Gerstner et al., 1996, Markram, 1997, Bi and Poo, 1998]. This form of plasticity, where the precise timing of spikes determines the subsequent synaptic changes, is named spike-timing-dependent plasticity (STDP) and is currently the most widely used learning rule in computational studies [Caporale and Dan, 2008, Morrison et al., 2008, Feldman, 2012]. Furthermore, the synaptic changes were shown to be additionally dependent on the rate of presynaptic and postsynaptic activity [Markram, 1997, Sjöström et al., 2001], postsynaptic depolarisation [Artola et al., 1990, Ngezahayo et al., 2000, Harvey and Svoboda, 2007], multiple pre- or postsynaptic spikes [Froemke and Dan, 2002, Wang et al., 2005, Nevian and Sakmann, 2006] and dendritic location of the synapse [Froemke et al., 2005, Sjöström and Häusser, 2006, Letzkus et al., 2006, Froemke et al., 2010]. These results have led to refined models for synaptic plasticity, among which are mechanistic models based on the calcium hypothesis [Shouval et al., 2002, Graupner and Brunel, 2012] and a voltage-dependent phenomenological model [Clopath et al., 2010] which we use in this study.

The STDP mechanism relies on the generation of action potentials and their subsequent backpropagation into the dendrites. These two requirements limit the capacity of STDP in the following cases. Firstly, STDP cannot account for activity-dependent learning with weak inputs, which are not powerful enough to evoke action potentials. Secondly, the attenuation or failure of the back-propagating action potential (bAP) provides a problem for STDP in the dendritic regions far from the soma [Froemke et al., 2005, Sjöström and Häusser, 2006, Letzkus et al., 2006]. Furthermore, an increasing number of experimental studies have revealed plasticity mechanisms which do not rely on postsynaptic action potential generation, but instead on local postsynaptic dendritic spikes [Golding et al., 2002, Kampa et al., 2006, Gordon et al., 2006, Gambino et al., 2014, Brandalise and Gerber, 2014, Kim et al., 2015, Cichon and Gan, 2015] or subthreshold events for dendritic spikes [Weber et al., 2016, Sandler et al., 2016]. The power of the STDP mechanism has since been highly debated [Lisman and Spruston, 2005, Hardie and Spruston, 2009, Lisman and Spruston, 2010, Schulz, 2010, Shouval et al., 2010, Frégnac et al., 2010, Buchanan and Mellor, 2010].

Taken together, these considerations indicate that pair-based STDP might only form part of the machinery a neuron offers, despite its prevalence in current theoretical works. Since the learning rules shape the connections in our brain, which ultimately affect the processing of information, it is crucial to understand which forms of plasticity are most prominent in neurons. In this article, we wondered how dendrites allow for multiple plasticity rules in a single cell. In a biophysical model of a cortical layer 2/3 pyramidal neuron, we implemented the voltage-based STDP rule (vSTDP, [Clopath et al., 2010]) which reproduces the various plasticity mechanisms described above [Artola et al., 1990, Markram, 1997, Ngezahayo et al., 2000, Sjöström et al., 2001, Froemke and Dan, 2002, Golding et al., 2002, Wang et al., 2005, Froemke et al., 2005, Sjöström and Häusser, 2006, Nevian and Sakmann, 2006, Letzkus et al., 2006, Harvey and Svoboda, 2007, Froemke et al., 2010, Gambino et al., 2014], and we focussed on the basal dendrites. Our simulations show a gradient of plasticity along these dendrites, with STDP dominating closer to the soma and a cooperative form of LTP closer to the tip of the dendrites. We then investigated the possible functional implications of these learning rules, showing how the plasticity mechanisms can interact to increase the neuron's flexibility and how stable associations can be learned.

RESULTS

We modelled a cortical layer 2/3 pyramidal neuron from primary visual cortex (V1). The reconstructed morphology of the neuron was taken from [Branco et al., 2010] (Figure 1a). We added Na^+, K^+ and Ca^{2+} conductances based on the fit to experimental data performed in [Acker and Antic, 2009] (see methods). All simulations were performed using Python with the Brian2 simulator [Goodman, 2008] and the code is available on ModelDB

(https://senselab.med.yale.edu/modeldb/). The synapses had both AMPA and NMDA components as in [Branco et al., 2010] and our model was able to reproduce the observed integration gradient along thin basal dendrites as reported in Branco and Häusser both experimentally and in a computational model [Branco and Häusser, 2011] (Figure 1b). This gradient was shown to arise from a difference in input impedance along the thin dendrites, resulting in greater depolarisation by single excitatory postsynaptic potentials (EPSPs) at locations closer to the tip of the dendrite compared to the soma. In turn, the higher depolarisation activates the supra-linear NMDA current. To avoid ambiguities in light of current literature, we point out to the reader that with *distal* we will denote the regions furthest from the soma on *basal* dendrites, as opposed to the apical tuft dendrites, and with *proximal* we mean the regions closer to the soma on *basal* dendrites, as opposed to the whole basal dendritic tree.

1/ Location dependence of local and global regenerative events

Dendrites allow for various local regenerative events, named dendritic spikes [Major et al., 2013]. Dendritic spikes in basal dendrites of cortical pyramidal neurons are usually evoked by the activation of NMDA receptor mediated channels, and called NMDA spikes [Gordon et al., 2006, Major et al., 2008, Antic et al., 2010]. We firstly investigate the NMDA-dependent integration gradient in our biophysical model: for each of the dendritic compartments, we recorded how many synapses need to be activated simultaneously to elicit either an NMDA or a somatic spike. We confirmed that synapses clustered on the dendritic compartments closer to the soma will result in the firing of a somatic spike before generating an NMDA spike, while synapses clustered on the dendritic compartments further from the soma elicit an NMDA spike without generating a somatic spike (Figure 1c). Moreover, the number of synapses needed to generate an NMDA spike is generally much lower than that for a somatic spike (Figure 1d). As these simulations were performed in the case where all synapses were placed in one compartment, we point out that distributing the synapses over multiple compartments would influence the generation of NMDA spikes but not action potentials (data not shown).

2/ Location dependence of STDP and cooperative plasticity

We wondered how the integration gradient described in the previous section affects synaptic plasticity. For this purpose, a local voltage-dependent STDP rule (vSTDP) was implemented in our model, based on [Clopath et al., 2010]. The rule can reproduce the depolarisation- and rate-dependence of plasticity [Artola et al., 1990, Ngezahayo et al., 2000, Markram, 1997, Sjöström et al., 2001, Harvey and Svoboda, 2007] (Figure 2b). We showed that our model is also consistent with experimental results reporting a reduced potentiation window for increasing distances from the soma, due to the attenuation of the back-propagating action potential (bAP) [Froemke et al., 2005, Sjöström and Häusser, 2006, Letzkus et al., 2006] (Figure 2c). Furthermore, we found that the same rule was able to account for local, dendritic-spike-dependent LTP, observed in vitro [Golding et al., 2002, Gordon et al., 2006, Kampa et al., 2006, Brandalise and Gerber, 2014, Weber et al., 2016] and in vivo [Gambino et al., 2014, Cichon and Gan, 2015]. Since vSTDP depends on voltage rather than postsynaptic spiking, a large postsynaptic depolarisation caused by a dendritic spike is sufficient for LTP and no bAP is required (Figure 2e). In the rest of the article, we will name this form of plasticity 'cooperative LTP'.

Since NMDA spikes are more easily evoked at the terminal regions of a dendrite (Figure 1), we investigated whether cooperative LTP, without the need for action potentials, is more easily evoked at distal locations. For this purpose, we stimulated 10 synapses either placed at the tip of a dendrite or at the initial compartment of the same dendrite. The synapses were all activated using a Poisson process with the same average rate. The synaptic group at the distal part of the

dendrite led to potentiation for substantially lower activation rates as opposed to the proximal group (Figure 2f). Our simulations show a plasticity gradient along basal dendrites: STDP is more effective in regions closer to the soma, while cooperative LTP is more easily evoked at distal regions. The latter mechanism could rescue the reduced potentiation in these regions caused by an attenuated bAP.

3/ Cooperative plasticity enables plasticity at weak, co-active inputs

In the previous section, we showed how STDP is less effective in the distal parts of the basal tree, while cooperative LTP is more easily evoked in these regions. Furthermore, the latter requires less inputs to trigger LTP compared to STDP-mediated LTP (Figure 2e). The cooperative LTP mechanism could therefore be used to strengthen inputs that are initially too weak to induce somatic spikes. We investigated this hypothesis by projecting groups of 5 synapses onto our morphological neuron model. The synapses in each group are co-activated, but the learning outcome depends on the synaptic configuration. Groups that were placed at a proximal compartment or randomly distributed across the basal dendritic tree did not undergo LTP (Figure 3, blue and green), whereas groups placed at the distal end of dendrites could lead to potentiation of the synapses, depending on the branch properties. Thin branches, that more easily allow for NMDA spikes, led to potentiation, whereas some thicker branches failed to elicit NMDA spikes and hence cooperative LTP (Figure 3, red). Our model shows that on the more distal regions of thin basal dendrites, weak co-active inputs can be strengthened even without postsynaptic spikes. Such a mechanism can be relevant to induce plasticity in silent neurons and hence engage them in the processing of stimuli, or similarly to induce changes in the representation of an active neuron.

4/ NMDA-dependent plateau potentials can gate plasticity at other synapses

The dendritic NMDA spikes are powerful regenerative events, with long plateau depolarisations lasting up to hundreds of milliseconds [Major et al., 2008, Antic et al., 2010]. As they are more easily evoked at the terminal regions of basal dendrites, they undergo substantial attenuation and cause only subthreshold events at the soma. The long subthreshold plateau does however enable other weak inputs to reach the spiking threshold, by reducing the required depolarisation to that threshold (Figure 4a).

We therefore asked whether the interaction between plateau potentials and subthreshold inputs affects plasticity. In particular, we explored the interplay between STDP and cooperative LTP by connecting three pools of synapses randomly across the basal dendrites. One extra group of synapses is added at the distal part of a thin branch (Figure 4b). The three pools are activated sequentially, but are too weak to induce potentiation by STDP. During the first half of the simulation, the activation of the first pool (Figure 4, brown) is coincident with the activation of the distal group (Figure 4, red). The weak inputs from the first pool paired with the plateau depolarisation now enable the neuron to elicit somatic spikes, which in turn lead to potentiation of synapses belonging to the first pool. During the second half of the simulation, the distal group is activated together with the second pool (Figure 4, yellow) instead of the first. The synapses belonging to the first pool depress again, while those from the second pool, now coupled with the plateau potential, are potentiated (Figure 4c).

These simulations show how the long-lasting plateau depolarisation caused by an NMDA spike can gate the plasticity at other synapses distributed across the dendritic tree. The distal group can therefore provide a teacher signal to the neuron, determining which inputs to learn. A neuron could exploit this interaction to flexibly change its input-output mapping without the need for a change in the rate of inputs. An additional feature is the increased temporal binding enabled by

the long-lasting nature of the NMDA spike (Figure 5b): we consider two groups of synapses and the activation of the second group is delayed with respect to the activation of the first group. The first group is either placed at a proximal or at a distal compartment, while the second, delayed group is distributed across the basal dendrites. To produce an action potential, the delay between the distal group and the distributed stimulus can be larger compared to the proximal case (Figure 5c,d). This increased time-window could be useful when associating inputs arriving from different pathways in the brain, for example associating multi-modal signals comprising of inputs from different senses, or associating bottom-up, sensory inputs arriving directly in primary cortical areas with top-down signals first processed in higher order areas and subsequently providing feedback in primary areas.

5/ Learning stable associations with cooperative LTP

We then sought to determine how the cooperative LTP affects the learning of associations. In the vSTDP rule, LTD depends on presynaptic activity and postsynaptic depolarisation (see methods). When a group of synapses is activated but fails to evoke a somatic or dendritic spike, the weights will be depressed. This situation can arise when activating only a fraction of associated inputs, leading to depression and in turn unlearning of the association. However, an association should be robust when presenting only its components, since neurons taking part in multiple assemblies and various sources of noise can lead to an incomplete activation. As the number of synapses needed for an action potential is larger than those needed for an NMDA spike (Figure 1d), we hypothesize that cooperative synapses allow for an increased retention of associations.

We developed this idea further in our detailed model. First, we activated two proximally grouped pools of neurons. We assume that the neuron should respond to the activation of both pools only, but not to the pools separately. For simplicity, the first pool is defined as coding for a circular shape and the second one for a blue color (Figure 6a). We further assume that we encounter many non-blue circular shapes and many non-circular blue objects, while only rarely observing blue circles. Hence, the separate activation of the circle-pool and the blue-pool will occur much more than the simultaneous activation of both pools (blue circle) (Figure 6b). Even though the simultaneous activations (blue circle) might elicit somatic spikes at the start of the simulation, the multitude of single-pool-activations will depress the involved synapses, ensuring that even simultaneously activating the pools eventually becomes subthreshold (Figure 6b,c). This poses a fundamental limit on learning cell-assemblies with similar STDP models.

In contrast, when two pools (circular shape and red color, Figure 6d) are located at the distal parts on basal dendrites, each activation of a pool elicits an NMDA spike, therefore keeping the synapses at the maximum weight (Figure 6e,f). Importantly, keeping the weights at full strength does not require any action potentials in this case, and the separate activations of each feature remain subthreshold and do not interfere. This allows the neuron to reliably produce output in the event of a red circle only (Figure 6e). Our example shows how cooperative LTP provides a mechanism to maintain associations between various inputs. Underlying this behaviour is a crucial difference between cooperative LTP and STDP. When using only STDP, the neuronal output also provides the learning signal for potentiation. Indeed, an action potential (output) is necessary for the induction of any weight change (learning). This is in stark contrast with cooperative LTP, where the potentiation is completely decoupled from the output (action potential generation) but instead relies on NMDA spikes. Therefore, the learning can happen independently from the output, allowing the different features of the learnt association to be activated separately without leading to depression.

Discussion

In our work, we propose that dendrites provide various plasticity mechanisms to a neuron, and their relative importance depends on the location of the synapse along the dendrite. We modelled a detailed multicompartmental neuron from [Branco et al., 2010] with active conductances, AMPA and NMDA mediated synapses, and a voltage-dependent plasticity rule [Clopath et al., 2010]. Our model confirms the experimentally observed plasticity compartments along single dendrites [Gordon et al., 2006, Weber et al., 2016] while providing a mechanistic understanding: the proximal region on basal dendrites, where the induction of dendritic NMDA-spikes is difficult [Major et al., 2008] and the innervation by back-propagating action potentials (bAPs) is most powerful [Nevian et al., 2007, Acker and Antic, 2009], favours STDP. The more distal regions favour local, cooperative LTP through the generation of NMDA-spikes but without the need for action potentials [Golding et al., 2002, Kampa et al., 2006, Gordon et al., 2006, Gambino et al., 2014, Brandalise and Gerber, 2014, Cichon and Gan, 2015]. This mechanism still allows for plasticity even when STDP fails, for example when the synapses are too weak to evoke action potentials.

Although homeostatic mechanisms could provide for similar strengthening of weak synapses, this is only achieved in an unspecific manner: when most inputs to a neuron are removed for a long period, all synapses will be strengthened simultaneously [Turrigiano and Nelson, 2004]. This is in contrast with the highly specific potentiation due to cooperative, nearby spines. While the generation of NMDA spikes are in principle required for this type of potentiation with the current model parameters, a recent study in hippocampus revealed cooperative LTP occurring without dendritic spikes [Weber et al., 2016]. To account for this type of potentiation, we would need to refine our plasticity rule. We point out that the resulting power of cooperative LTP relative to STDP would be further increased, as even less synaptic inputs would be required by the former, and therefore the results would not change qualitatively. The cooperative form of plasticity could be additionally gated by brain-derived neurotrophic factor (BDNF), as observed in [Gordon et al., 2006].

Another requirement for cooperative LTP is the spatial proximity of co-active synapses. The typical length along which calcium signals spread and cooperative plasticity can occur, is around 10-20 microns [Schiller et al., 2000, Weber et al., 2016]. This indicates that the functional plasticity units of a neuron are on this scale, in agreement with in vivo calcium activity in dendrites [Hill et al., 2013]. It is however unclear to what extent functional synaptic clusters are present on dendrites [Harvey and Svoboda, 2007, Fu et al., 2012, Druckmann et al., 2014, Jia et al., 2010, Chen et al., 2011]. As this form of potentiation would need as few as 2 to 4 synapses within 20 microns of dendritic length [Weber et al., 2016], and considering a spine density of about 1-1.5 spines per micron in human cortical basal dendrites [Benavides-Piccione et al., 2013], such clusters do not need to be apparent and neighbouring spines can easily form synapses from distinct signals: different clusters can be intertwined and can mingle with unclustered synapses. In order to arrange synapses with the necessary spatial proximity, structural plasticity might play an additional important role [Fu et al., 2012]. Indeed, similar synaptic arrangements have been achieved in theoretical models by a combination of cooperative and structural plasticity in [Mel, 1991, Poirazi and Mel, 2001].

We further showed how dendritic spikes provide a plateau depolarisation in the soma, which in turn enables other weak inputs to reach the spiking threshold. In this way, the more distally located cooperative inputs can gate the plasticity at other synapses. Such an interplay can enhance the flexibility of a neuron, where the strengthening and weakening of synapses depends on the coincidence with a dendritic spike acting as a teacher signal, allowing changes to be reversed. Similar mechanisms, where inputs on a region of the dendritic tree can control the plasticity at a distinct area have been reported in hippocampus [Dudman et al., 2007, Takahashi and Magee,

2009, Brandalise and Gerber, 2014] and explored in theoretical models [Urbanczik and Senn, 2014]. Moreover, it was shown that the modulation of gain curves between different regions on a single branch is asymmetric and location dependent [Behabadi et al., 2012], revealing a complex interplay between distal and proximal inputs. Finally, we provided an example of how a neuron can use cooperative LTP to maintain learnt associations, which would otherwise be depressed by an STDP mechanism. From a dynamical systems perspective, the plasticity rules have distinct stable points, all of which can now be exploited by the neuron. Taken together, these results indicate that different regions on the dendritic tree allow for non-trivial interactions, enriching the computational potential of a neuron.

In this study, we did not consider various other plasticity mechanisms: intrinsic and homeostatic plasticity [Triesch, 2007, Turrigiano, 2011, Turrigiano, 2012, Yger and Gilson, 2015], structural plasticity [Caroni et al., 2012], heterosynaptic plasticity [Chistiakova et al., 2014, Chistiakova et al., 2015] and branch strength plasticity [Losonczy et al., 2008, Makara et al., 2009, Legenstein and Maass, 2011]. Moreover, we only considered basal dendrites, and the apical tuft dendrites might give rise to a new learning rules [Kim et al., 2015, Sandler et al., 2016], especially in cortical layer 5 pyramidal neurons which are known to possess a powerful calcium spike initiation zone in this region [Schiller et al., 1997]. Understanding these plasticity mechanisms can provide further insight into the interaction of bottom-up inputs arriving on the basal dendrites and top-down feedback arriving at the tuft. Furthermore, we neglected inhibitory synapses, which are known to target specific regions of the dendritic tree [Markram et al., 2004, Bloss et al., 2016] and affect the neuronal output in a location-dependent way [Jadi et al., 2012].

In the present article, we focussed on plasticity across the basal dendrites and how it affects the computational capabilities of a single-cell. However, it is unclear how the different plasticity compartments in a neuron shape the network dynamics and connectivity. For example, it is known that connectivity between neurons is not random: data from V1 indicates that intra-laminar recurrent connectivity shows above chance levels of bidirectional connectivity, favouring strong connections between neurons with similar orientation selectivity and hence strongly correlated activity [Ko et al., 2011, Ko et al., 2013, Cossell et al., 2015]. It would be interesting to investigate whether a level of specificity also exists across the basal dendritic tree, perhaps with feedforward sensory inputs providing the majority of the cooperative distal inputs, where learning is decoupled from the output, and recurrent connections providing mostly distributed synapses, where STDP is the main learning mechanism and hence input-output correlations are crucial. To address these questions, we propose the possibility to use networks containing reduced multicompartmental neurons, with dendrites comprising of one proximal and one distal compartment. Similar simplified models with reduced dendrites have been used previously, highlighting the advantage of dendrites for computational purposes [Legenstein and Maass, 2011, Behabadi et al., 2012, Jadi et al., 2012, Cazé et al., 2012, Urbanczik and Senn, 2014, Thalmeier et al., 2016, Brea et al., 2016].

To conclude, our simulations indicate that STDP only partially contributes to the learning mechanisms in a neuron. We showed that in the distal regions on basal dendrites, a small amount of synapses can cooperate to elicit NMDA spikes and trigger LTP. Therefore, dendrites not only allow for various non-linear interactions between EPSPs, they also provide different synaptic plasticity rules, enriching learning and increasing the possible robust input to output mappings.

Methods

For all simulations, we used the Brian2 neuron simulator [Goodman, 2008] in Python. The codes will be posted on ModelDB (https://senselab.med.yale.edu/modeldb/) after publication.

Neuron Morphology and passive properties

We used a morphological reconstruction of a Layer 2/3 pyramidal neuron of mouse visual cortex, reconstructed by Branco et al. [Branco et al., 2010]. The HOC file was converted into an SWC file using the free software NLMorphologyConverter (http://neuronland.org/NLMorphologyConverter/NLMorphologyConverter.html). For this purpose, the original soma (21 compartments) was replaced by a single-compartment spherical soma with approximately the same volume (radius of the sphere = 8 µm). The total number of compartments in the model was 488.

The passive parameters for the neuron were:

Timestep	dt	25 µs
Leak conductance	g_L	$\mathrm{mS\,cm^{-2}}$
Leak potential	E_L	-69.5 mV
Membrane capacitance	C_m	$1\ \mu\mathrm{F\,cm^{-2}}$
Axial resistance	R_a	90 Ω cm

To account for spines, we increase the leak conductance and membrane capacitance by factor of 1.5 for distances larger than 50 microns, as in [Acker and Antic, 2009]. The value of E_L was chosen to ensure a resting potential of the neuron of -75 mV.

Ion channels

The active conductances in our model were adapted from [Acker and Antic, 2009], a study in which a fit was made to match experimental data on action potential backpropagation in basal dendrites of layer 5 pyramidal cells. The most prominent differences between layer 5 and layer 2/3 pyramidal neurons are found in the apical dendrites: the Ca^{2+}-spike initiation zone and Ih current are almost completely absent in layer 2/3 neurons [Waters et al., 2003, Larkum et al., 2007, Palmer et al., 2014]. These results indicate that the apical tuft dendrites of layer 2/3 neurons might be more similar to the basal dendrites. Nevertheless we chose to distribute synapses solely across the basal dendritic tree in all our simulations.

We further modified the distribution of the channels in the soma and axon from [Acker and Antic, 2009] in order to have a spike initiation in the initial part of the axon instead of the soma. All equations governing the channel dynamics were identical as in [Acker and Antic, 2009], but translated from the HOC files into python with Brian2. As in [Acker and Antic, 2009], most temperature dependencies are removed from the ion conductances, except for the high-threshold calcium channel. The conductance of the latter should therefore be multiplied by a factor of 2.11 for a fair comparison with other conductances, as we used a temperature of 32 degrees Celsius. We point out that in most models with the NEURON simulator, the conductances are temperature dependent, which one should take into account when comparing with the current work. Full details on the ion channel dynamics and distributions can be found in [Acker and Antic, 2009], a summary of the ion channel distributions in our model can be found in the tables below. For simplicity, we will use the following abbreviations:

- Voltage-gated Na^+ channels : Na_v
- Delayed-rectifier K^+ channels: K_v
- A-type K^+ channel: Ka_v
- High-threshold Ca^{2+} channels: Cah_v
- Low-threshold Ca^{2+} channels: Cal_v

Soma

Na_v	200 pS µm^{-2}
K_v	400 pS µm^{-2}
Ka_v (proximal type)	300 pS µm^{-2}
Cah_v	4 pS µm^{-2}
Cal_v	1 pS µm^{-2}

Basal dendrites

Sodium and potassium channel densities linearly depend on the distance d to the soma in microns.

Na_v	(150 - 0.5*d*µm^{-1}) pS µm^{-2}
K_v	40 pS µm^{-2}
Ka_v	(150 + 0.7*d*µm^{-1}) pS µm^{-2}
Cah_v	0.4 pS µm^{-2}
Cal_v	0.1 pS µm^{-2}

Apical dendrites

Na_v	250 pS µm^{-2}
K_v	40 pS µm^{-2}
Ka_v	300 pS µm^{-2}
Cah_v	0.4 pS µm^{-2}
Cal_v	0.1 pS µm^{-2}

The Ka_v channel density in all dendrites is further divided into proximal and distal A-type potassium channels (full details in [Acker and Antic, 2009]).

Axon

In order to mimic spike initiation in the axon, the initial two segments of the axon have increasing K_v density (40 and 100 pS µm^{-2}) and decreasing Na_v density (8000 and 7000 pS µm^{-2}). The rest of the axon has a constant K_v density of 500 pS µm^{-2} and Na_v density of 5000 pS µm^{-2}. There are no calcium conductances in the axon, except in the first two compartments where the calcium conductances have the same values as in the soma. Additionally, a low-threshold activated, slowly inactivating potassium current is added in the first four compartments of the axon, and is zero otherwise.

Synapses

Synapses consist of both AMPA and NMDA channels. The maximal conductance of NMDA receptors is always double of the AMPA conductance, as was used in [Branco and Häusser, 2011] to reproduce the integration gradient along dendrites. This ratio is within the observed experimental range [Watt et al., 2000]. An activated synapse will result in an instantaneous rise of both AMPA and NMDA conductances by an amount of $g = w \cdot g_{\max}$, where w is the synaptic

weight and $g_{\max}$ is the maximal conductance for either AMPA or NMDA. This is followed by an exponential decay with the respective time-constants for AMPA and NMDA:

$$\tau_{\text{AMPA/NMDA}} \frac{dg(t)}{dt} = -g(t) + w \cdot g_{\max} \cdot \delta(t - t_f)$$

$\delta(x)$ is the Dirac delta function, t_f is the presynaptic firing time and $\tau_{\text{AMPA/NMDA}}$ is the synaptic time constant of AMPA or NMDA receptors. The current flowing through AMPA receptors is modelled by

$$I_{\text{AMPA}} = g(t) \cdot (v - E_{\text{AMPA}})$$

while the NMDA current is given by

$$I_{\text{NMDA}} = g(t) \cdot B(v) \cdot (v - E_{\text{NMDA}})$$

$B(v)$ describes the voltage-dependence of the magnesium block in NMDA channels [Jahr and Stevens, 1990],

$$B(v) = \frac{1}{1 + \frac{\exp(-0.062 \cdot v)}{3.57}}$$

All parameters are below:

AMPA time-constant	τ_{AMPA}	2 ms
AMPA reversal potential	E_{AMPA}	0 mV
NMDA time-constant	τ_{NMDA}	50 ms
NMDA reversal potential	E_{NMDA}	0 mV
maximal AMPA conductance	g_{AMPA}	1.5 nS
maximal NMDA conductance	g_{NMDA}	3 nS

Plasticity

The plasticity rule used is based on the voltage-based STDP rule from Clopath et al. [Clopath et al., 2010] without homeostasis, where the synaptic weights w_i follow

$$\frac{dw_i(t)}{dt} = -A_{LTD} X_i \left(\bar{u}_-(t) - \theta_-\right)_+ + A_{LTP} \bar{x}_i(t) \left(u(t) - \theta_+\right)_+ \left(\bar{u}_+(t) - \theta_-\right)_+$$

with

$$\begin{aligned}
\tau_x \frac{d\bar{x}_i(t)}{dt} &= -\bar{x}_i(t) + X_i(t) \\
\tau_- \frac{d\bar{u}_-(t)}{dt} &= -\bar{u}_-(t) + \bar{u}_1(t) \\
\tau_+ \frac{d\bar{u}_+(t)}{dt} &= -\bar{u}_+(t) + \bar{u}_1(t) \\
\tau_1 \frac{\bar{u}_1(t)}{dt} &= -\bar{u}_1(t) + u(t)
\end{aligned}$$

The extra low-pass filter $\bar{u}_1$ is implemented to introduce a small delay in the low-pass filters $\bar{u}_+$ and $\bar{u}_-$, which was achieved in the original model by filtering $u(t-\epsilon)$. The voltage $u(t)$ in each compartment is generated by the Brian2 simulator.

We refer the reader to [Clopath et al., 2010] for full details and give a short summary here: this rule has a depression term and a potentiation term. The term responsible for potentiation incorporates a presynaptic spike train X_i and the low-pass filtered postsynaptic depolarisation $(\bar{u}_- - \theta_-)_+$. The $(\cdot)_+$ stands for rectification, i.e. the term is only non-zero if the number within the brackets is positive. $\bar{u}_-$ is a low-pass filtered version of the membrane potential with time constant τ_-, and θ_- is a threshold for synaptic plasticity. To summarize, this term states that a presynaptic spike will lead to depression if the postsynaptic membrane is depolarised, for example because the postsynaptic neuron fired a spike in the recent past. An isolated post-pre pairing will therefore lead to depression. The term responsible for potentiation includes a low-pass filtered presynaptic spike train $\bar{x}_i$, a low-pass filtered postsynaptic depolarisation $(\bar{u}_+ - \theta_-)_+$ and an instantaneous depolarisation above a potentiation threshold $(u - \theta_+)_+$. The time constant for the low-pass filtered version of the membrane potential $\bar{u}_+$ is given by τ_+. The potentiation threshold θ_+ is high enough to be selective for back-propagating action potentials or NMDA spikes. Potentiation can therefore occur when a postsynaptic spike happens after a presynaptic neuron fired and while the postsynaptic membrane is depolarised, for example because the postsynaptic neuron fired another spike in the recent past as well. Potentiation is therefore possible when there are triplets of spikes (pre-post-post or post-pre-post), which can occur as isolated triplets or during a sustained high rate firing. Secondly, potentiation can occur when an NMDA spike (also called dendritic plateau potential) is generated. These plateau potentials provide a long and sufficiently high depolarisation, leading to potentiation without generating postsynaptic action potentials. The above equations ensure all-to-all plasticity. The parameters are fitted to reproduce the frequency dependence of plasticity, as previously done by [Clopath et al., 2010]:

lowpass filter timeconstant 1	τ_1	5 ms
lowpass filter timeconstant 2	τ_-	15 ms
lowpass filter timeconstant 3	τ_+	45 ms
Depolarization threshold for plasticity	Θ_-	-74.3 mV
Depolarization threshold for potentiation	Θ_+	-15 mV
Spike trace reset value	x_{reset}	5
Spike trace timeconstant	τ_x	20 ms
Depression amplitude	A_{LTD}	3.5e-4
Potentiation amplitude	A_{LTP}	17.5e-4

In all simulations, the minimum and maximum weight for the synapses were 0.1 and 1 respectively, unless stated otherwise. The choice of Θ_+, the threshold for potentiation, was made by comparing data from [Sjöström and Häusser, 2006] with [Acker and Antic, 2009]. In the former, it is shown how the attenuation of the bAP results in a transition from potentiation to depression at a distance of about 200 μm, while in the latter it is shown that the bAP amplitude at this distance is about 60 mV above the resting potential (-75 mV in our case).

Simulations

Figure 1

Fig 1b: From a basal dendrite, a synapse at the maximum weight was connected to the nearest and most distant compartment relative to the soma. The synapse was activated 10 times, with an interspike interval of 1ms, 4ms or 8ms. The membrane potential at the soma was stored.

Fig 1c,d: For each compartment in our morphological neuron (except soma and axonal compartments), a number of synapses was activated with interspike interval of 1ms and the local membrane voltage was recorded during the subsequent 15ms. The number of synapses was increased until a threshold at -15mV was crossed. By comparing the local voltage with the somatic voltage, it was determined whether this threshold was crossed due to an NMDA spike or a somatic spike. The number of synapses needed to reach this threshold was stored.

Fig 2

Figure 2a: In the same compartments as for Figure 1, either the distal or the proximal synapse is activated reproducing the experimental protocol in [Sjöström et al., 2001]. Pairs of pre-post or post-pre spikes separated by 10ms are repeated five times at different frequencies of 1,10,25,40 and 50 Hz. The weight change is multiplied by a factor of 15 to mimic the experimental protocol in [Sjöström et al., 2001]. The initial synaptic weights are 0.5 and the weight change after the six pairings are plotted in function of the frequency.

Figure 2b: The same pairing protocol as in figure 2a at 20Hz was repeated for different interspike intervals (1,5,10 and 20ms).

Figure 2c: The synapse in the distal compartment, as in Figure 1b, is activated 10 times with an interspike interval of 0.1ms.

Figure 2d: Either the proximal or the distal compartment as in Figure 1 is connected with 10 synapses, all with an initial weight of 0.5. The synapses are activated using a Poisson process with the same average rate, lasting 200ms. This protocol is repeated with rates various from 1Hz to 60Hz.

Fig 3

Fifteen groups of 10 synapses are connected to the morphological neuron. The first five groups are each connected to a distal compartment on the basal tree, the second five each to a proximal compartment and synapses from the final five groups are distributed randomly across the basal dendrites. Each group is activated during 15ms by generating Poisson-distributed spikes with an average rate of 300 Hz at the every synapse belonging to the group. Subsequent activations were separated by a 200ms interval. Initial weights were all 0.3. A single activation of one group for each synaptic configuration is shown in Figure 3b. Each group is activated twice and the average weight of synapses in a group is shown with a circle in Figure 3c.

Fig 4

Three input pools with 10 synapses each are randomly distributed across the basal dendrites, initiated at the minimum weight. Five extra synapses are clustered at a distal compartment on a basal dendrite. These synapses are initiated at the maximum weight and will be paired with one of the other input pools. The activation of the pools or the distal cluster comprises of activating the relevant synapses during 250ms at an average rate of 50Hz. Subsequent activations of pools were separated by a 200ms interval.

During the first half of the simulation (0s-22.5s), the activations of the first pool are paired with the activation of the distal cluster. During the second half of the simulation (22.5s-45s), the second pool is paired with the cluster. In order to observe the depression when a pool is not paired with the cluster, the maximum weight is reduced to 0.65 instead of 1. The minimum weight is increased from 0.1 to 0.55, enabling the weakest synapses to still reach the spiking threshold when paired

with the cluster. To compensate for the reduced range between the minimum and maximum weight, the amplitudes $A_L TD$ and $A_L TP$ for depression and potentiation are one third of the usual values described above.

Fig 5

Two groups of 15 synapses are connected to the neuron, initialised at the maximum weight 1. For the first pool, all synapses are clustered onto one compartment. For the second, synapses are randomly distributed across the basal dendrites. The distributed group is activated synchronously, but with a delay (0ms up to 75ms) relative to the clustered group, also activated synchronously.

Fig 6

Two pools of 4 neurons are connected to proximal compartments on basal dendrites (synapses of the same pool are clustered onto the same compartment). The initial weights are at the maximum hard bound 1, and an additional coloured noisy current is injected in the soma:

$$\frac{dI_{\text{noise}}}{dt} = \frac{(\mu_{\text{noise}} - I_{\text{noise}})}{\tau_{\text{noise}}} + \xi\sigma_{\text{noise}}\sqrt{\frac{2}{\tau_{\text{noise}}}}$$

with standard deviation $\sigma_{\text{noise}} = 25\text{pA}$, mean $\mu_{\text{noise}} = 100\text{pA}$ and $\tau_{\text{noise}} = 20\text{ms}$ is the time-constant for the low-pass filtering of the Gaussian white noise with zero mean and unit standard deviation $\xi(t)$. The pools are activated sequentially, with an active pool comprising of Poisson-distributed spikes at an average rate of 30Hz at the member synapses during 350ms. Two subsequent activations are separated by a 150ms interval. Every 10 activations (i.e. 5 for each pool), both pools are activated simultaneously.

References

[Acker and Antic, 2009] Acker, C. D. and Antic, S. D. (2009). Quantitative assessment of the distributions of membrane conductances involved in action potential backpropagation along basal dendrites. *Journal of neurophysiology*, 101(3):1524–1541.

[Antic et al., 2010] Antic, S. D., Zhou, W. L., Moore, A. R., Short, S. M., and Ikonomu, K. D. (2010). The decade of the dendritic NMDA spike. *Journal of Neuroscience Research*, 88(14):2991–3001.

[Artola et al., 1990] Artola, a., Bröcher, S., and Singer, W. (1990). Different voltage-dependent thresholds for inducing long-term depression and long-term potentiation in slices of rat visual cortex.

[Behabadi et al., 2012] Behabadi, B. F., Polsky, A., Jadi, M., Schiller, J., and Mel, B. W. (2012). Location-dependent excitatory synaptic interactions in pyramidal neuron dendrites. *PLoS computational biology*, 8(7):e1002599.

[Benavides-Piccione et al., 2013] Benavides-Piccione, R., Fernaud-Espinosa, I., Robles, V., Yuste, R., and Defelipe, J. (2013). Age-based comparison of human dendritic spine structure using complete three-dimensional reconstructions. *Cerebral Cortex*, 23(8):1798–1810.

[Berlucchi and Buchtel, 2009] Berlucchi, G. and Buchtel, H. A. (2009). Neuronal plasticity: Historical roots and evolution of meaning. *Experimental Brain Research*, 192(3):307–319.

[Bi and Poo, 1998] Bi, G. Q. and Poo, M. M. (1998). Synaptic modifications in cultured hippocampal neurons: dependence on spike timing, synaptic strength, and postsynaptic cell type. *The Journal of neuroscience : the official journal of the Society for Neuroscience*, 18(24):10464–10472.

[Bienenstock et al., 1982] Bienenstock, E. L., Cooper, L. N., and Munro, P. W. (1982). Theory for the development of neuron selectivity: orientation specificity and binocular interaction in visual cortex. *The Journal of neuroscience : the official journal of the Society for Neuroscience*, 2(1):32–48.

[Bliss and Lømo, 1973] Bliss, T. V. P. and Lømo, T. (1973). Long-lasting potentiation of synaptic transmission in the dentate area of the anaesthetized rabbit following stimulation of the perforant path. *The Journal of Physiology*, 232(2):331–356.

[Bloss et al., 2016] Bloss, E. B., Cembrowski, M. S., Karsh, B., Colonell, J., Fetter, R. D., and Spruston, N. (2016). Structured Dendritic Inhibition Supports Branch-Selective Integration in CA1 Pyramidal Cells. *Neuron*, 89(5):1–15.

[Branco et al., 2010] Branco, T., Clark, B. a., and Häusser, M. (2010). Dendritic discrimination of temporal input sequences in cortical neurons. *Science (New York, N.Y.)*, 329(5999):1671–5.

[Branco and Häusser, 2011] Branco, T. and Häusser, M. (2011). Synaptic integration gradients in single cortical pyramidal cell dendrites. *Neuron*, 69(5):885–92.

[Brandalise and Gerber, 2014] Brandalise, F. and Gerber, U. (2014). Mossy fiber-evoked subthreshold responses induce timing-dependent plasticity at hippocampal CA3 recurrent synapses. *Proceedings of the National Academy of Sciences of the United States of America*, 111(11):4303–8.

[Brea et al., 2016] Brea, J., Gaál, A. T., Urbanczik, R., and Senn, W. (2016). Prospective Coding by Spiking Neurons. *PLOS Computational Biology*, 12(6):e1005003.

[Buchanan and Mellor, 2010] Buchanan, K. A. and Mellor, J. R. (2010). The activity requirements for spike timing-dependent plasticity in the hippocampus. *Frontiers in Synaptic Neuroscience*, 2(JUN):1–5.

[Caporale and Dan, 2008] Caporale, N. and Dan, Y. (2008). Spike timing-dependent plasticity: a Hebbian learning rule. *Annual review of neuroscience*, 31:25–46.

[Caroni et al., 2012] Caroni, P., Donato, F., and Muller, D. (2012). Structural plasticity upon learning: regulation and functions. *Nature Reviews Neuroscience*, 13(7):478–490.

[Cazé et al., 2012] Cazé, R., Humphries, M., and Gutkin, B. (2012). Spiking and saturating dendrites differentially expand single neuron computation capacity. *Nips*, pages 1–9.

[Chen et al., 2011] Chen, X., Leischner, U., Rochefort, N. L., Nelken, I., and Konnerth, A. (2011). Functional mapping of single spines in cortical neurons in vivo. *Nature*, 475(7357):501–505.

[Chistiakova et al., 2014] Chistiakova, M., Bannon, N. M., Bazhenov, M., and Volgushev, M. (2014). Heterosynaptic Plasticity: Multiple Mechanisms and Multiple Roles. *The Neuroscientist*, 20(5):483–498.

[Chistiakova et al., 2015] Chistiakova, M., Bannon, N. M., Chen, J.-Y., Bazhenov, M., and Volgushev, M. (2015). Homeostatic role of heterosynaptic plasticity: models and experiments. *Frontiers in computational neuroscience*, 9(July):89.

[Cichon and Gan, 2015] Cichon, J. and Gan, W.-B. (2015). Branch-specific dendritic Ca2+ spikes cause persistent synaptic plasticity. *Nature*, 520(7546):180–5.

[Clopath et al., 2010] Clopath, C., Büsing, L., Vasilaki, E., and Gerstner, W. (2010). Connectivity reflects coding: a model of voltage-based STDP with homeostasis. *Nature neuroscience*, 13(3):344–52.

[Cossell et al., 2015] Cossell, L., Iacaruso, M. F., Muir, D. R., Houlton, R., Sader, E. N., Ko, H., Hofer, S. B., and Mrsic-flogel, T. D. (2015). Functional organization of excitatory synaptic strength in primary visual cortex. *Nature*, 518(7539):399–403.

[Druckmann et al., 2014] Druckmann, S., Feng, L., Lee, B., Yook, C., Zhao, T., Magee, J., and Kim, J. (2014). Structured Synaptic Connectivity between Hippocampal Regions. *Neuron*, 81(3):629–640.

[Dudek and Bear, 1992] Dudek, S. M. and Bear, M. F. (1992). Homosynaptic long-term depression in area CA1 of hippocampus and effects of N-methyl-D-aspartate receptor blockade. *Proceedings of the National Academy of Sciences of the United States of America*, 89(10):4363–7.

[Dudman et al., 2007] Dudman, J. T., Tsay, D., and Siegelbaum, S. A. (2007). A Role for Synaptic Inputs at Distal Dendrites: Instructive Signals for Hippocampal Long-Term Plasticity. *Neuron*, 56(5):866–879.

[Feldman, 2012] Feldman, D. E. D. (2012). The spike-timing dependence of plasticity. *Neuron*, 75(4):556–571.

[Frégnac et al., 2010] Frégnac, Y., Pananceau, M., René, A., Huguet, N., Marre, O., Levy, M., and Shulz, D. E. (2010). A re-examination of Hebbian-covariance rules and spike timing-dependent plasticity in cat visual cortex in vivo. *Frontiers in Synaptic Neuroscience*, 2(DEC):1–21.

[Froemke and Dan, 2002] Froemke, R. C. and Dan, Y. (2002). Spike-timing-dependent synaptic modification induced by natural spike trains. *Nature*, 416(6879):433–438.

[Froemke et al., 2010] Froemke, R. C., Letzkus, J. J., Kampa, B. M., Hang, G. B., and Stuart, G. J. (2010). Dendritic synapse location and neocortical spike-timingdependent plasticity. *Frontiers in Synaptic Neuroscience*, (JUL).

[Froemke et al., 2005] Froemke, R. C., Tsay, I. A., Raad, M., Long, J. D., and Dan, Y. (2005). Contribution of Individual Spikes in Burst-Induced Long-Term Synaptic Modification. *J Neurophysiol*, 95:1620–1629.

[Fu et al., 2012] Fu, M., Yu, X., Lu, J., and Zuo, Y. (2012). Repetitive motor learning induces coordinated formation of clustered dendritic spines in vivo. *Nature*, 483(7387):92–5.

[Gambino et al., 2014] Gambino, F., Pagès, S., Kehayas, V., Baptista, D., Tatti, R., Carleton, A., and Holtmaat, A. (2014). Sensory-evoked LTP driven by dendritic plateau potentials in vivo. *Nature*, 515(V):116–119.

[Gerstner et al., 1996] Gerstner, W., Kempter, R., van Hemmen, J. L., and Wagner, H. (1996). A neuronal learning rule for sub-millisecond temporal coding. *Nature*, 383(6595):76–78.

[Golding et al., 2002] Golding, N. L., Staff, N. P., and Spruston, N. (2002). Dendritic spikes as a mechanism for cooperative long-term potentiation. *Nature*, 418(6895):326–331.

[Goodman, 2008] Goodman, D. (2008). Brian: a simulator for spiking neural networks in Python. *Frontiers in Neuroinformatics*, 2(November):1–10.

[Gordon et al., 2006] Gordon, U., Polsky, A., and Schiller, J. (2006). Plasticity compartments in basal dendrites of neocortical pyramidal neurons. *The Journal of neuroscience : the official journal of the Society for Neuroscience*, 26(49):12717–12726.

[Graupner and Brunel, 2012] Graupner, M. and Brunel, N. (2012). Calcium-based plasticity model explains sensitivity of synaptic changes to spike pattern, rate, and dendritic location. *Proceedings of the National Academy of Sciences*, 109(10):3991–3996.

[Hardie and Spruston, 2009] Hardie, J. and Spruston, N. (2009). Synaptic Depolarization Is More Effective than Back-Propagating Action Potentials during Induction of Associative Long-Term Potentiation in Hippocampal Pyramidal Neurons. *Journal of Neuroscience*, 29(10):3233–3241.

[Harvey and Svoboda, 2007] Harvey, C. D. and Svoboda, K. (2007). Locally dynamic synaptic learning rules in pyramidal neuron dendrites. *Nature*, 450(7173):1195–1200.

[Hebb, 1949] Hebb, D. O. (1949). The Organization of Behavior. *The Organization of Behavior*, 911(1):335.

[Hill et al., 2013] Hill, D. N., Varga, Z., Jia, H., Sakmann, B., and Konnerth, A. (2013). Multibranch activity in basal and tuft dendrites during firing of layer 5 cortical neurons in vivo. *Proceedings of the National Academy of Sciences*, 110(33):13618–13623.

[Jadi et al., 2012] Jadi, M., Polsky, A., Schiller, J., and Mel, B. W. (2012). Location-Dependent Effects of Inhibition on Local Spiking in Pyramidal Neuron Dendrites. *PLoS Computational Biology*, 8(6):e1002550.

[Jahr and Stevens, 1990] Jahr, C. E. and Stevens, C. F. (1990). Voltage dependence of NMDA-activated macroscopic conductances predicted by single-channel kinetics. *The Journal of neuroscience : the official journal of the Society for Neuroscience*, 10(9):3178–3182.

[Jia et al., 2010] Jia, H., Rochefort, N. L., Chen, X., and Konnerth, A. (2010). Dendritic organization of sensory input to cortical neurons in vivo. *Nature*, 464(7293):1307–1312.

[Kampa et al., 2006] Kampa, B. M., Letzkus, J. J., and Stuart, G. J. (2006). Requirement of dendritic calcium spikes for induction of spike-timing-dependent synaptic plasticity. *The Journal of physiology*, 574(Pt 1):283–90.

[Kim et al., 2015] Kim, Y., Hsu, C.-L., Cembrowski, M. S., Mensh, B. D., and Spruston, N. (2015). Dendritic sodium spikes are required for long-term potentiation at distal synapses on hippocampal pyramidal neurons. *eLife*, 4:1–30.

[Ko et al., 2013] Ko, H., Cossell, L., Baragli, C., Antolik, J., Clopath, C., Hofer, S. B., and Mrsic-Flogel, T. D. (2013). The emergence of functional microcircuits in visual cortex. *Nature*, 496(7443):96–100.

[Ko et al., 2011] Ko, H., Hofer, S. B., Pichler, B., Buchanan, K. a., Sjöström, P. J., and Mrsic-Flogel, T. D. (2011). Functional specificity of local synaptic connections in neocortical networks. *Nature*, 473(7345):87–91.

[Larkum et al., 2007] Larkum, M. E., Waters, J., Sakmann, B., and Helmchen, F. (2007). Dendritic spikes in apical dendrites of neocortical layer 2/3 pyramidal neurons. *The Journal of neuroscience : the official journal of the Society for Neuroscience*, 27(34):8999–9008.

[Legenstein and Maass, 2011] Legenstein, R. and Maass, W. (2011). Branch-specific plasticity enables self-organization of nonlinear computation in single neurons. *The Journal of neuroscience : the official journal of the Society for Neuroscience*, 31(30):10787–802.

[Letzkus et al., 2006] Letzkus, J. J., Kampa, B. M., and Stuart, G. J. (2006). Learning Rules for Spike Timing-Dependent Plasticity Depend on Dendritic Synapse Location. *Journal of Neuroscience*, 26(41):10420–10429.

[Lisman and Spruston, 2005] Lisman, J. and Spruston, N. (2005). Postsynaptic depolarization requirements for LTP and LTD: a critique of spike timing-dependent plasticity. *Nature neuroscience*, 8(7):839–841.

[Lisman and Spruston, 2010] Lisman, J. and Spruston, N. (2010). Questions about STDP as a general model of synaptic plasticity. *Frontiers in Synaptic Neuroscience*, 2(OCT):1–5.

[Losonczy et al., 2008] Losonczy, A., Makara, J. K., and Magee, J. C. (2008). Compartmentalized dendritic plasticity and input feature storage in neurons. *Nature*, 452(7186):436–41.

[Major et al., 2013] Major, G., Larkum, M. E., and Schiller, J. (2013). Active properties of neocortical pyramidal neuron dendrites. *Annual review of neuroscience*, 36:1–24.

[Major et al., 2008] Major, G., Polsky, A., Denk, W., Schiller, J., and Tank, D. W. (2008). Spatiotemporally graded NMDA spike/plateau potentials in basal dendrites of neocortical pyramidal neurons. *Journal of Neurophysiology*, 99(5):2584–2601.

[Makara et al., 2009] Makara, J. K., Losonczy, A., Wen, Q., and Magee, J. C. (2009). Experience-dependent compartmentalized dendritic plasticity in rat hippocampal CA1 pyramidal neurons. *Nature neuroscience*, 12(12):1485–7.

[Markram, 1997] Markram, H. (1997). Regulation of Synaptic Efficacy by Coincidence of Postsynaptic APs and EPSPs. *Science*, 275(5297):213–215.

[Markram et al., 2004] Markram, H., Toledo-Rodriguez, M., Wang, Y., Gupta, A., Silberberg, G., and Wu, C. (2004). Interneurons of the neocortical inhibitory system. *Nature Reviews Neuroscience*, 5(10):793–807.

[Mel, 1991] Mel, B. W. (1991). The clusteron: Toward a simple abstraction for a complex neuron. *Nips*, pages 35–42.

[Morrison et al., 2008] Morrison, A., Diesmann, M., and Gerstner, W. (2008). Phenomenological models of synaptic plasticity based on spike timing. *Biological Cybernetics*, 98(6):459–478.

[Nevian et al., 2007] Nevian, T., Larkum, M. E., Polsky, A., and Schiller, J. (2007). Properties of basal dendrites of layer 5 pyramidal neurons: a direct patch-clamp recording study. *Nature neuroscience*, 10(2):206–14.

[Nevian and Sakmann, 2006] Nevian, T. and Sakmann, B. (2006). Spine Ca2+ Signaling in Spike-Timing-Dependent Plasticity. *Journal of Neuroscience*, 26(43):11001–11013.

[Ngezahayo et al., 2000] Ngezahayo, a., Schachner, M., and Artola, a. (2000). Synaptic activity modulates the induction of bidirectional synaptic changes in adult mouse hippocampus. *The Journal of neuroscience : the official journal of the Society for Neuroscience*, 20(7):2451–2458.

[Palmer et al., 2014] Palmer, L. M., Shai, A. S., Reeve, J. E., Anderson, H. L., Paulsen, O., and Larkum, M. E. (2014). NMDA spikes enhance action potential generation during sensory input. *Nature neuroscience*, 17(3):383–90.

[Poirazi and Mel, 2001] Poirazi, P. and Mel, B. W. (2001). Impact of active dendrites and structural plasticity on the memory capacity of neural tissue. *Neuron*, 29(3):779–796.

[Sandler et al., 2016] Sandler, M., Shulman, Y., and Schiller, J. (2016). A Novel Form of Local Plasticity in Tuft Dendrites of Neocortical Somatosensory Layer 5 Pyramidal Neurons. *Neuron*, 90(5):1028–1042.

[Schiller et al., 2000] Schiller, J., Major, G., Koester, H. J., and Schiller, Y. (2000). NMDA spikes in basal dendrites of cortical pyramidal neurons. *Nature*, 404(6775):285–289.

[Schiller et al., 1997] Schiller, J., Schiller, Y., Stuart, G., and Sakmann, B. (1997). Calcium action-potentials restricted to distal apical dendrites of rat neocortical pyramidal neurons. *J. Physiol.*, 505:605–616.

[Schulz, 2010] Schulz, J. M. (2010). Synaptic plasticity in vivo: More than just spike-timing? *Frontiers in Synaptic Neuroscience*, 2(NOV):1–2.

[Shouval et al., 2002] Shouval, H. Z., Bear, M. F., and Cooper, L. N. (2002). A unified model of NMDA receptor-dependent bidirectional synaptic plasticity. *Proceedings of the National Academy of Sciences*, 99(16):10831–10836.

[Shouval et al., 2010] Shouval, H. Z., Wang, S. S.-H., and Wittenberg, G. M. (2010). Spike timing dependent plasticity: a consequence of more fundamental learning rules. *Frontiers in computational neuroscience*, 4(July):1–13.

[Sjöström and Häusser, 2006] Sjöström, P. J. and Häusser, M. (2006). A Cooperative Switch Determines the Sign of Synaptic Plasticity in Distal Dendrites of Neocortical Pyramidal Neurons. *Neuron*, 51(2):227–238.

[Sjöström et al., 2001] Sjöström, P. J., Turrigiano, G. G., and Nelson, S. B. (2001). Rate, Timing, and Cooperativity Jointly Determine Cortical Synaptic Plasticity. *Neuron*, 32(6):1149–1164.

[Stent, 1973] Stent, G. S. (1973). A physiological mechanism for Hebb's postulate of learning. *Proceedings of the National Academy of Sciences of the United States of America*, 70(4):997–1001.

[Takahashi and Magee, 2009] Takahashi, H. and Magee, J. C. (2009). Pathway Interactions and Synaptic Plasticity in the Dendritic Tuft Regions of CA1 Pyramidal Neurons. *Neuron*, 62(1):102–111.

[Thalmeier et al., 2016] Thalmeier, D., Uhlmann, M., Kappen, H. J., and Memmesheimer, R.-M. (2016). Learning Universal Computations with Spikes. *PLOS Computational Biology*, 12(6):e1004895.

[Triesch, 2007] Triesch, J. (2007). Synergies Between Intrinsic and Synaptic Plasticity Mechanisms. *Neural Computation*, 19(4):885–909.

[Turrigiano, 2011] Turrigiano, G. (2011). Too many cooks? Intrinsic and synaptic homeostatic mechanisms in cortical circuit refinement. *Annual review of neuroscience*, 34:89–103.

[Turrigiano, 2012] Turrigiano, G. (2012). Homeostatic synaptic plasticity: Local and global mechanisms for stabilizing neuronal function. *Cold Spring Harbor Perspectives in Biology*, 4(1):1–18.

[Turrigiano and Nelson, 2004] Turrigiano, G. G. and Nelson, S. B. (2004). Homeostatic plasticity in the developing nervous system. *Nature reviews. Neuroscience*, 5(2):97–107.

[Urbanczik and Senn, 2014] Urbanczik, R. and Senn, W. (2014). Learning by the dendritic prediction of somatic spiking. *Neuron*, 81(3):521–8.

[Wang et al., 2005] Wang, H.-X., Gerkin, R. C., Nauen, D. W., and Bi, G.-Q. (2005). Coactivation and timing-dependent integration of synaptic potentiation and depression. *Nature Neuroscience*, 8(2):187–193.

[Waters et al., 2003] Waters, J., Larkum, M., Sakmann, B., and Helmchen, F. (2003). Supralinear Ca2+ influx into dendritic tufts of layer 2/3 neocortical pyramidal neurons in vitro and in vivo. *The Journal of neuroscience : the official journal of the Society for Neuroscience*, 23(24):8558–8567.

[Watt et al., 2000] Watt, a. J., van Rossum, M. C., MacLeod, K. M., Nelson, S. B., and Turrigiano, G. G. (2000). Activity coregulates quantal AMPA and NMDA currents at neocortical synapses. *Neuron*, 26(3):659–670.

[Weber et al., 2016] Weber, J. P., Andrásfalvy, B. K., Polito, M., Magó, Á., Ujfalussy, B. B., and Makara, J. K. (2016). Location-dependent synaptic plasticity rules by dendritic spine cooperativity. *Nature Communications*, 7:11380.

[Yger and Gilson, 2015] Yger, P. and Gilson, M. (2015). Models of Metaplasticity: A Review of Concepts. *Frontiers in Computational Neuroscience*, 9(November):1–14.

Acknowledgements

We like to thank Romain Cazé for providing a script for visualising the neuron morphology and Wilten Nicola for comments on an earlier version of the manuscript.

Author Contributions

J.B. and C.C. planned the research and wrote the paper, J.B. performed the numerical computations.

Figures

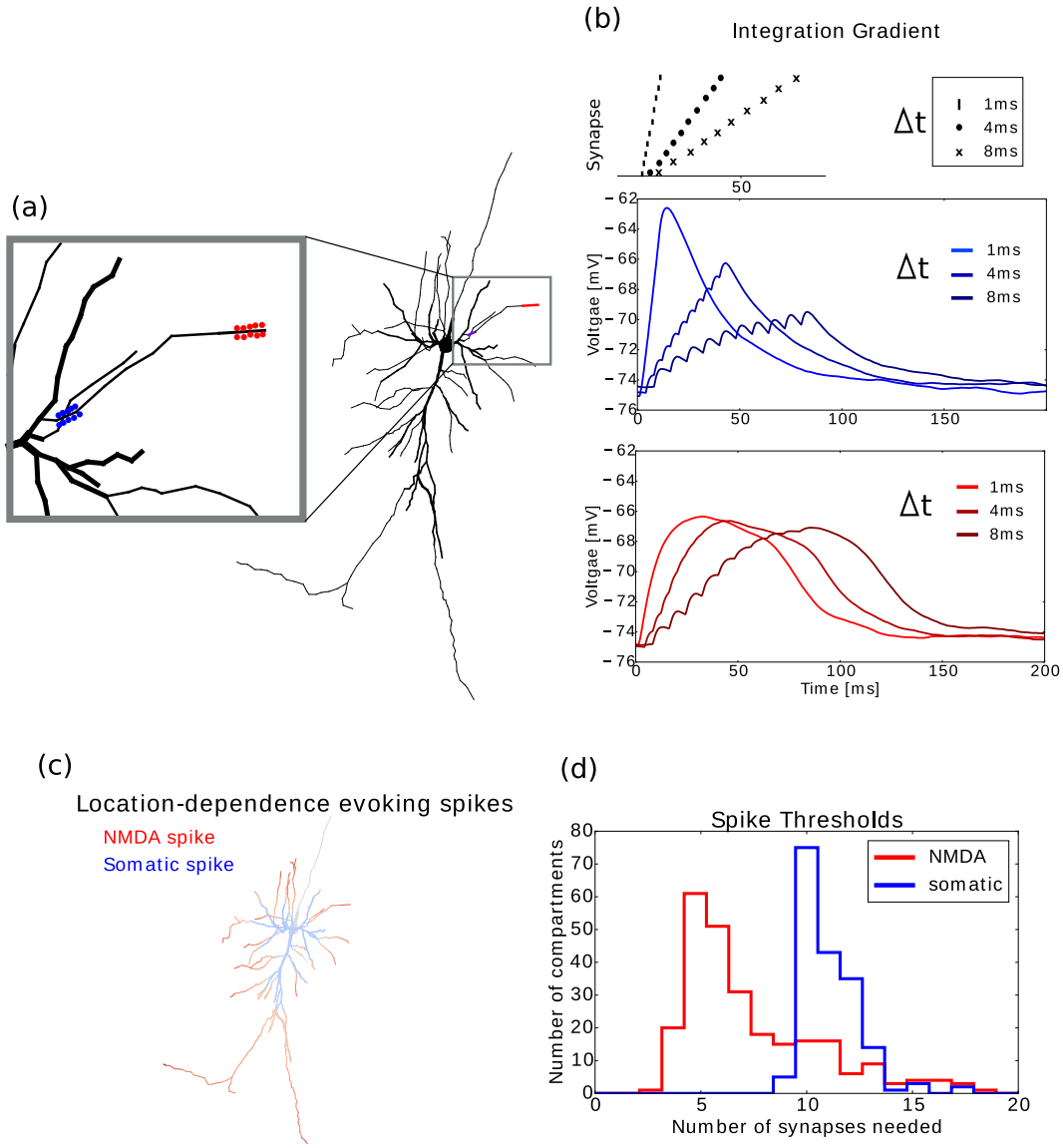

Figure 1 Location dependence of local and global regenerative events.
(**a**) Proximal (blue) and distal (red) location on a thin basal branch of the detailed neuron model. (**b**) Temporal integration gradient along a basal dendrite (as observed in [Branco and Häusser, 2011]). Top panel: activation sequences with different interspike intervals. Middle panel: proximal stimulation requires high temporal coincidence, as the somatic depolarisation drops substantially when inputs are not active synchronously. Bottom panel: distal stimulation results in similar somatic depolarisation for a bigger range of interspike intervals. (**c**) For each dendritic compartment in the neuron model, synapses are activated until either an NMDA spike or an action potential is generated. Stimulating proximal compartments results in an action potential before reaching the threshold for NMDA spikes (blue). Stimulating distal regions results in NMDA spike generation while staying subthreshold for somatic spikes (red). Intenser colors denote that less synapses are needed to evoke a spike. (**d**) For each compartment in (c), the number of synapses needed to evoke the spikes was stored and represented as a histogram. NMDA spikes (red) generally require around 5 activated synapses in our model, while somatic spikes (blue) require around 10 synapses.

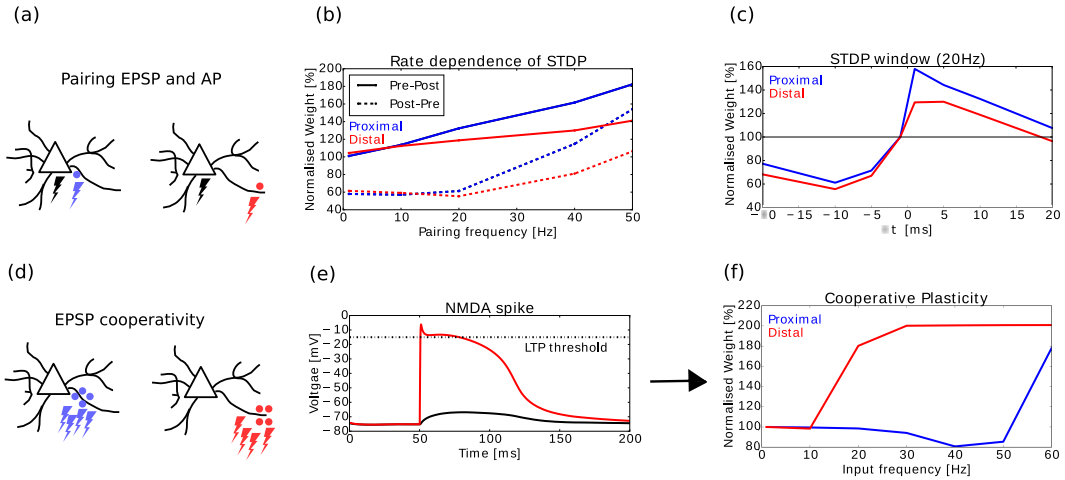

Figure 2 Plasticity gradient along basal dendrites.
(**a**) Action potentials (black lightning) is paired with either proximal (blue) or distal (red) synaptic activations. (**b**) The pairing protocol as in [Sjöström et al., 2001] is simulated. Action potentials and EPSPs are paired with a fixed interval of 10ms, either pre-post (full lines) or post-pre (dashed lines). The pairings are repeated $15 \cdot 5$ times at a fixed frequency (see methods). The protocol is repeated for several pairing frequencies (horizontal axis) and the normalised weight change is displayed (vertical axis). The experimentally observed rate-dependence is reproduced, where low rates lead to depression only, intermediate rates allow for both potentiation and depression depending on the spike timings, and high rates lead to potentiation only. Distal synapses show less potentiation due to the attenuation of the bAP. (**c**) The same protocol as in (b) is repeated at a pairing frequency of 20 Hz, but the interspike interval is now varied (horizontal axis). The normalised weight change (vertical axis) shows the standard STDP window, with a reduced window for potentiation at distal synapses due to the attenuation of the bAP. (**d**) A group of synapses on a proximal compartment (blue) or distal compartment (red) are activated by a Poisson process. (**e**) Distal groups of synapses can elicit NMDA spikes (red trace), which cross the LTP threshold of the plasticity model and can therefore result in potentiation while remaining subthreshold in the soma (black trace). (**f**) When activating the synaptic groups as in (d), LTP is observed at much lower average activation rates for the distal group (red trace) compared to the proximal group (blue trace). This local, cooperative LTP by NMDA spikes compensates for the lack of potentiation by STDP (b,c).

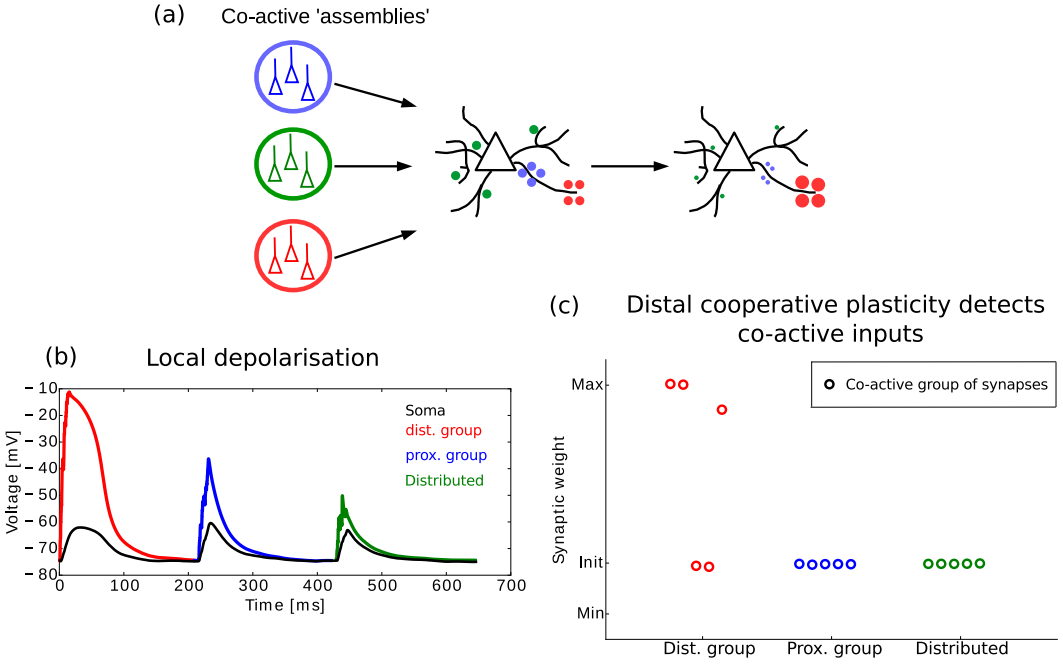

Figure 3 Co-active synapses are detected by distal clusters.
(**a**) Three types of co-active synapses are wired to our neuron: proximally grouped synapses (blue), randomly distributed synapses (green) and distally grouped synapses (red). Only distal groups lead to potentiation. (**b**) The activation of the different groups leads to subthreshold responses in the soma for all cases (black trace), but NMDA spikes can be generated for distal groups (red trace). (**c**) The synaptic weight after stimulation (vertical axis) shows potentiation only for distal groups. Note that some thicker dendritic branches require more inputs to elicit NMDA spikes and don't show potentiation.

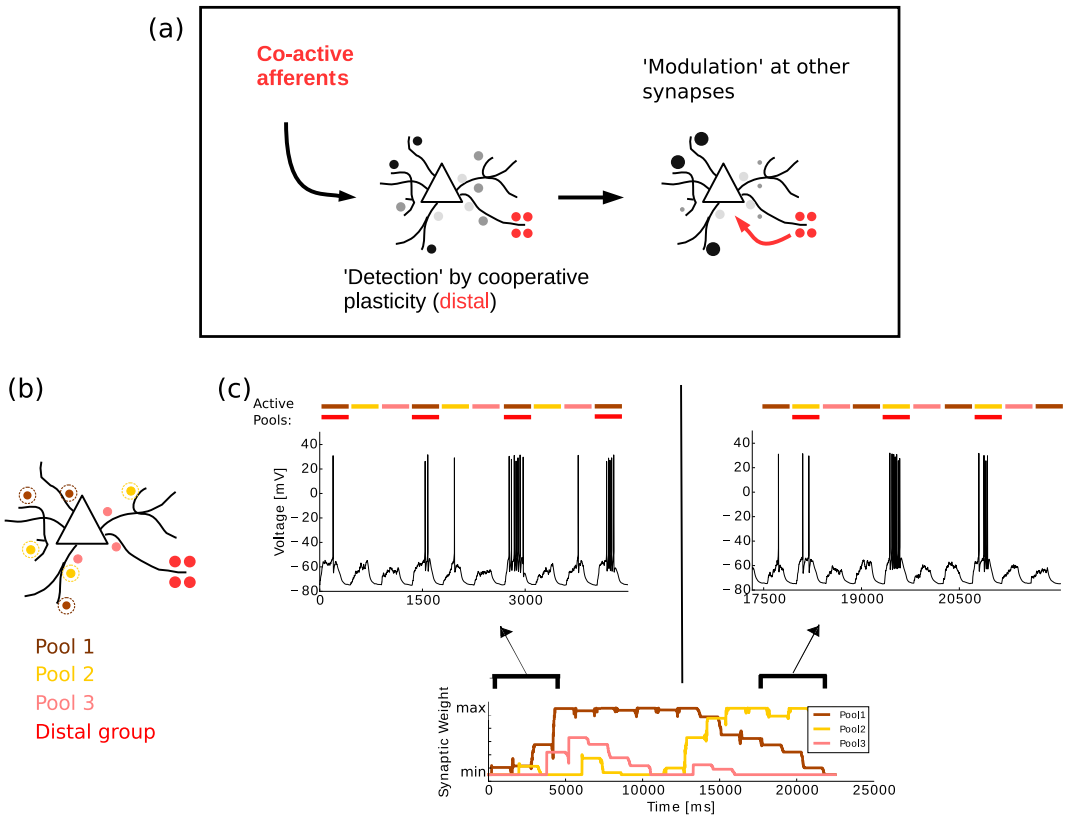

Figure 4 Distally evoked plateau potentials can gate plasticity at other synapses.
(**a**) Cartoon of the hypothesis that the distally potentiated clusters, as in Figure 3, can in turn modulate plasticity at other locations. (**b**) Different synaptic groups are connected to the neuron: three pools (brown, yellow, pink) are randomly distributed across the basal dendrites, and one group (red) is connected on one distal compartment. (**c**) Top panel, left: the distal cluster (red) is paired with pool 1 (brown) in the first part of the simulation. The neuron almost exclusively reaches the spiking threshold when these synapses are active together. This leads to potentiation of the brown synapses (bottom panel, first part). Top panel, right: the distal cluster (red) is paired with pool 2 (yellow) in the second part of the simulation. The brown synapses depress again and the yellow synapses potentiate (bottom panel, second part).

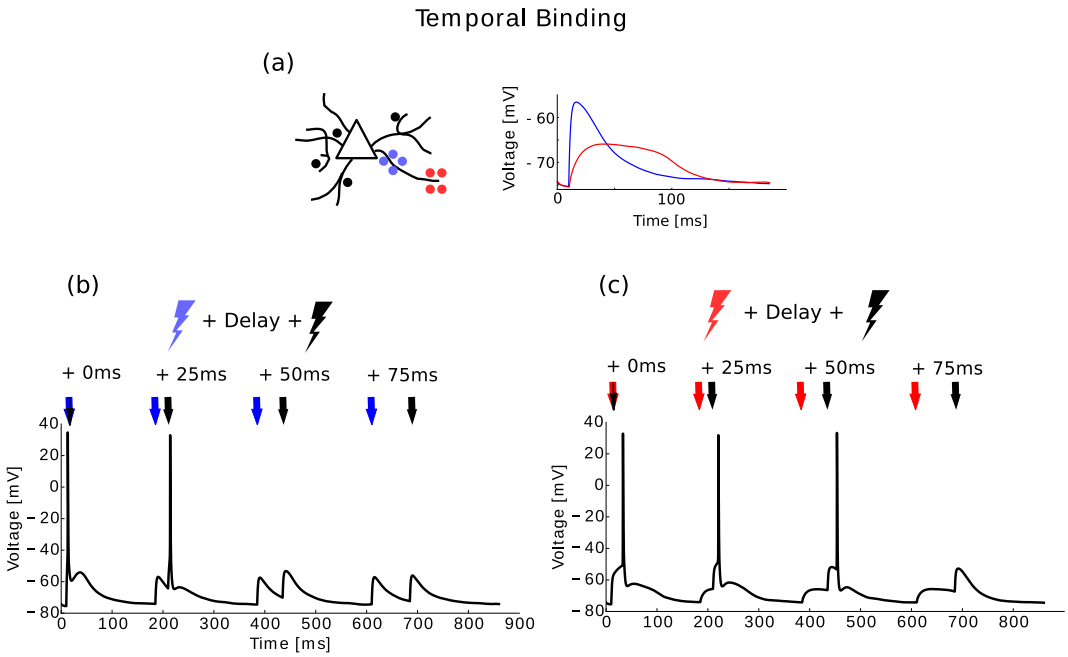

Figure 5 Plateau potentials increase the time window for associations.
(**a**) Left: cartoon of synaptic arrangements, with a distributed group of synapses (black), a proximally connected group (blue) and a distally connected group (red). Right: activation of the distal group leads to a longer-lasting plateau in the soma (red) compared to proximal activation (blue). (**b**) The proximal group is activated, followed by a delayed activation of the distributed group. Action potentials are evoked for delays up to 25 ms. (**c**) The same protocol as in (b), but with the distal group instead of the proximal one, leads to action potentials with delays up to 50 ms.

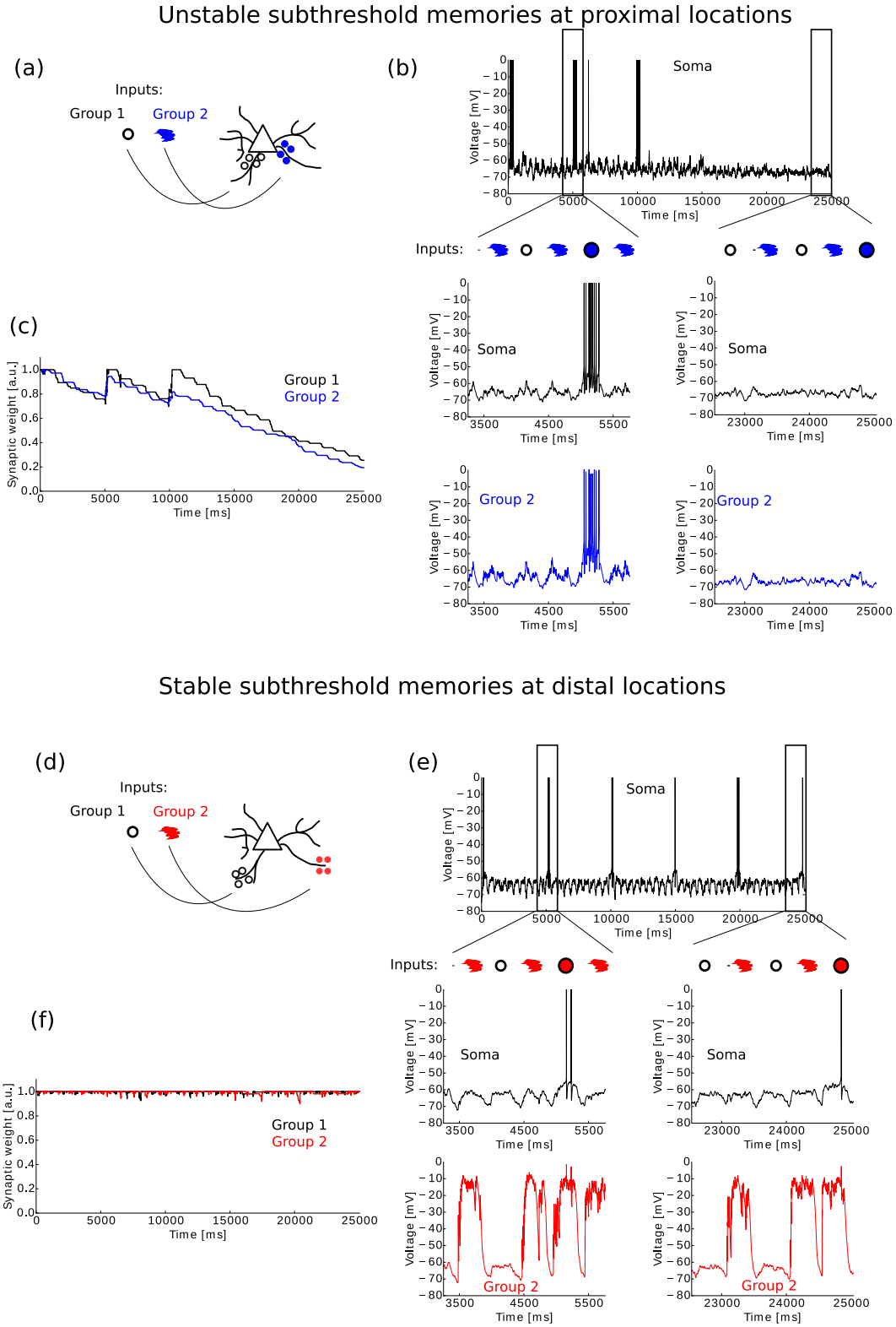

Figure 6 Novel stable associations allowed by cooperative LTP.
(caption continued on next page)

(continued from previous page) (**a**) Cartoon of the simulation: two groups of synapses are placed at proximal compartments. Group 1 codes for a circle, group 2 for the colour blue. While the groups are often activated separately, the neuron should only generate an output in the rare event of a blue circle (i.e. both groups active simultaneously). (**b**) Top panel: somatic trace during the simulation. Middle panels: detail of the somatic trace during initial half and final half of the simulation. While a blue circle leads to action potentials initially, it eventually becomes subthreshold. Bottom panels: dendritic traces at the proximal location of cluster 2, corresponding to the somatic traces in the middle panel. (**c**) Evolution of synaptic weights of both groups during the simulation. The individual activations of the groups lead to depression, the simultaneous activations result in potentiation initially, but insufficient to keep the synapses at the maximum weight. Finally, the simultaneous activations become subthreshold and the weights depress towards the lower bound. (**d,e,f**) Analogous to (a,b,c), but connecting the groups at distal locations on basal dendrites. The individual activations of the groups now lead to NMDA spikes (see panel e, bottom, for the second group), keeping the weights at the upper bound (panel f) and allowing the neuron to maintain its red-circle representation (panel e, top and middle).